A multi-scale approach for the simultaneous shape and material optimisation of sandwich panels with cellular core

Marco Montemurro*
Arts et Métiers ParisTech, I2M CNRS UMR 5295, F-33400 Talence, France.

Anita Catapano
Bordeaux INP, Université de Bordeaux, I2M CNRS UMR 5295, F-33400 Talence, France

Dominique Doroszewski
Arts et Métiers ParisTech, F-33400 Talence, France

Author for Correspondence:
Marco Montemurro, PhD,
Arts et Métiers ParisTech,
I2M CNRS UMR 5295,
F-33400 Talence, France,
tel: +33 55 68 45 422,
fax: +33 54 00 06 964,
e.mail: marco.montemurro@ensam.eu,
marco.montemurro@u-bordeaux1.fr

*Corresponding author.

Abstract

This work deals with the problem of the optimum design of a sandwich panel made of carbon-epoxy skins and a metallic cellular core. The proposed design strategy is a multi-scale numerical optimisation procedure that does not make use of any simplifying hypothesis to obtain a true global optimum configuration of the system. To face the design of the sandwich structure at both meso and macro scales, a two-level optimisation strategy is employed: at the first level the goal is the determination of the optimum shape of the unit cell of the core (meso-scale) together with the material and geometric parameters of the laminated skins (macro-scale), while at the second level the objective is the design of the skins stacking sequence (skin meso-scale) meeting the geometrical and material parameters provided by the first-level problem. The two-level strategy is founded on the polar formalism for the description of the anisotropic behaviour of the laminates, on the NURBS basis functions for representing the shape of the unit cell and on the use of a genetic algorithm as optimisation tool to perform the solution search. To prove its effectiveness, the multi-scale strategy is applied to the least-weight design of a sandwich plate subject to constraints of different nature: on the positive-definiteness of the stiffness tensor of the core, on the admissible material properties of the laminated faces, on the local buckling load of the unit cell, on the global buckling load of the panel and geometrical as well as manufacturability constraints related to the fabrication process of the cellular core.

Keywords:

Honeycomb; Laminates; Buckling; Computational modelling; Shape optimisation.

1 Introduction

Sandwich panels are increasingly used in aerospace, automotive and naval industries thanks to their high stiffness-to-weight and strength-to-weight ratios. In order to further reduce the weight of these structures, sandwich panels are made by laminated skins separated by aluminium or resin honeycombs, or by polymer foams whose material and geometrical properties can be designed to provide sandwich plates with enhanced mechanical properties (stiffness, strength, etc.). However, the design process and the subsequent optimisation of sandwich structures presents several difficulties mainly when the panel is made of laminated skins and a honeycomb core. In this case the designer has to face, into the same design process, both the difficulty of designing a laminated plate (concerning the skins) and that of designing a complex 3D cellular continuum such as the honeycomb core. Therefore, engineers always make use of some simplifying assumptions or rules to obtain, in an easy and fast way, a solution. For example, in [1, 2, 3] the optimal design of a sandwich plate is addressed by determining exclusively the optimum thickness of both the core and the skins, keeping constant the rest of geometric and material parameters of the system. In [4] the authors deal with the problem of the least-weight design of a sandwich plate considering as design variables the thickness of the cell walls as well as that of the skins together with the total height of the panel. They employed an analytical model to evaluate both the buckling load of the core and the faces yielding which were considered as optimisation constraints.

The optimisation problem was solved using a Genetic Algorithm (GA). A step further in the formulation of the problem of the optimum design of sandwich structures has been done by introducing the concept of topology optimisation of periodic structures. For example, in [5] Neves *et al.* present two computational models for predicting the topology of periodic microstructures which optimise the equivalent material properties determined through a numerical homogenisation technique. Barbarosie and Toader [6] derive analytically the shape and topological derivatives for elliptic problems in unbounded domains subject to periodicity conditions. In [7] Wadley *et al.* compare different topologies of sandwich cores in order to evaluate their structural performance along with the most suited fabrication process. In this work the classical configurations of sandwich cores such as foams or honeycombs are questioned and the authors show how new shapes of the repetitive unit cell, obtained through an optimisation process, can lead to more efficient solutions (i.e. lighter and stiffer). In [8] Huang and Xie present a method for the topology optimisation of periodic structures using the bi-directional evolutionary structural optimisation technique. The capability and the effectiveness of their approach is demonstrated through some numerical applications on sandwich structures.

The study presented in this work can be placed within the framework of the research activities [9, 10] previously conducted by the authors and can be seen as a generalisation of these works.

In [9, 10] a very general multi-scale procedure for the optimum design of sandwich panels with a hexagonal honeycomb core is proposed. The design problem is formulated without introducing simplifying hypotheses and by considering (as design variables) the full set of geometric and material parameters defining the behaviour of the structure at each characteristic scale (meso and macro). The design variables are the geometric parameters of the hexagonal unit cell (meso-scale) together with the geometric and material parameters of the laminated skins (meso and macro scales). To deal with the multi-scale design problem of a sandwich plate a two-level optimisation strategy is employed. At the first level of the procedure the optimum value of the cell parameters along with the material and geometrical properties of the laminated skins are determined (at this level each skin is modelled as an equivalent homogeneous anisotropic plate whose mechanical behaviour at the macro-scale is described through a set of tensor invariants, i.e. the laminate polar parameters [11]). At the second level of the strategy the goal is to find at least one stack for each skin (thus the design variables of this phase are the plies orientation angles) meeting the optimum combination of their material and geometrical parameters resulting from the first level of the procedure.

The aim of the present work is twofold. On one hand the formulation of the design problem of the sandwich panel is generalised by considering the shape optimisation of the unit cell of the core instead of the classical size optimisation of a prescribed geometry (as

done in [9, 10] for the hexagonal unit cell). On the other hand the two-level optimisation procedure has been enriched by considering the manufacturability constraints linked to the fabrication process of the unit cell within the first level of the strategy. In order to fabricate in an easy and fast way a prototype of the cellular core a 3D printing technique has been considered as a fabrication process. Concerning the geometry of the cellular core, the shape of the unit cell is described by means of B-spline and Non-Uniform Rational B-Spline (NURBS) curves [12]. The utilisation of B-spline and NURBS bases allows for easily translating the manufacturability constraints (due to the additive manufacturing process) into geometrical constraints to be imposed on the geometry of the representative unit cell. Moreover, since the first level of the strategy involves two different scales (the macro-scale of the sandwich panel and the meso-scale of the cellular core) the meso-scale 3D finite element model of the repetitive unit cell of the core presented in [9] (which is used to evaluate its effective elastic properties at the macro-scale) has been geenralised in order to take into account for the variation of the shape of the cell. The whole procedure is based on the utilisation of the polar formalism [13] as well as on a genetic algorithm (GA) previously developed by the first author [14]. The paper is organised as follows: the design problem, the two-level strategy and the rapid prototyping technique used for fabricating the cellular core are discussed in Section 2. The mathematical formulation of the first-level problem is detailed in Section 3, while the problem of determining a suitable laminate is formulated in Section 4. A concise description of the Finite Element (FE) models of the sandwich structure at both meso and macro scales are given in Section 5, while the numerical results of the optimisation procedure are shown in Section 6. Finally, Section 7 ends the paper with some concluding remarks.

2 Simultaneous shape and material optimisation of sandwich panels with cellular core

2.1 Description of the problem

The optimisation strategy presented in this study is applied to a sandwich plate composed of two laminated skins and a metallic cellular core with *free-shape* cells as depicted in Figs. 1 and 2. The skins are made of carbon-epoxy unidirectional orthotropic laminae while the cellular core is obtained from aluminium alloy foils, see Table 1 for the material properties taken from [15, 16]. Concerning the cellular core, the basic classical assumptions considered to evaluate its elastic response and, hence, to determine its effective material properties (at the macro-scale) are:

- linear, elastic behaviour for the material of the cell walls;
- perfect bonding for the wall-to-wall contact;

- the buckling of the cell walls due to shear stresses is disregarded.

Concerning the mechanical behaviour (at the macro-scale) of the identical laminated skins, they are modelled as quasi-homogeneous fully orthotropic laminates, see Section 3.2. As discussed in [10], no simplifying hypotheses are made on the geometric and mechanical parameters of both skins and core. Only avoiding the utilisation of a priori assumptions that extremely shrink the solution space (e.g. the utilisation of symmetric balanced stacks for the laminated faces to attain membrane/bending uncoupling and membrane orthotropy, respectively, or the utilisation of regular hexagonal cells to reduce the number of optimisation variables for the core) one can hope to obtain the true global optimum for a given problem: this is a key-point in our approach.

Finally, in this work the problem formulation has been enriched by including the shape optimisation of the unit cell of the cellular core (which is not fixed a priori) as well as the manufacturability constraints linked to the fabrication process of the periodic structure of the core.

2.2 Description of the multi-scale two-level optimisation strategy

The main goal of the design strategy is the least-weight design of the sandwich plate subject to constraints of different nature, i.e. mechanical, geometrical as well as feasibility and manufacturability constraints. The optimisation procedure is articulated into the following two distinct (but linked) optimisation problems.

First-level problem. The aim of this phase is the determination of the optimal shape of the unit cell together with the material and geometric parameters of the laminated skins in order to minimise the weight of the structure and to satisfy, simultaneously, the full set of optimisation constraints. At this level the laminate representing each skin is modelled as an equivalent homogeneous anisotropic plate whose behaviour at the macro-scale is described in terms of the laminate polar parameters, see [10]. Concerning the model of the cellular core, the first-level problem involves two different scales: the meso-scale of the repetitive unit cell characterised by its geometric variables, as well as the macro-scale where the core itself is modelled as an homogeneous orthotropic solid. The link between these two scales, as widely described in [9], is represented by the homogenisation phase of the cellular core.

Second-level problem. At the second level of the strategy, the goal is the determination of a suitable lay-up for both skins (the skin meso-scale) meeting the optimum combination of their material and geometrical parameters provided by the first level problem. The aim of this phase is, hence, to find at least one stacking sequence, for each skin, which has to be quasi-homogeneous, fully orthotropic and that has to satisfy the optimal values of the polar parameters resulting from the first step. At this level of the strategy, the design variables are the layer orientations.

2.3 Rapid prototyping of the optimum configurations

Thanks to the development of more and more forefront fabrication techniques, the process of additive manufacturing has shown in recent years a rapid development. Among the advantages provided by this technique, the most important concerns the ability of reproducing objects of complex shape without (or with less) restrictive technological constraints linked to the process itself. Since in our laboratory we do not yet dispose of an additive manufacturing machine for fabricating structural elements made of aluminium alloy, we decided to employ a 3D printing technique to manufacture the prototype of the optimised configuration of the cellular core of the sandwich panel. This fact is not limiting because the aim here is not to reproduce the "real" structural element, rather we want to prove that a new design paradigm can be conceived: a true global optimisation of the sandwich structure can be carried out only by including both shape and material optimisation aspects within the design process. Furthermore, it is possible to obtain realistic (i.e. manufacturable) complex shapes of the cellular core only if the technological constraints linked to the fabrication process are taken into account since the early stages of the design process.

The 3D printer employed to fabricate the prototypes is the Objet30 Pro of Stratasys [17], while the material employed for the cellular core structure is the VeroWhite FullCure830 belonging to the Objet's FullCure Materials family of acrylic-based photopolymer materials [18].

3 Mathematical formulation of the first-level problem

The overall characteristics of the structure have to be designed during this phase. The weight minimisation of the sandwich plate will be performed by satisfying the set of optimisation constraints listed below:

- a constraint on the global buckling load of the sandwich panel;
- a constraint on the local buckling load of the repetitive unit cell;
- the manufacturability constraints linked to the considered fabrication process;
- a geometric constraint imposed on the shape of the unit cell for avoiding overlapping of the middle-line of the cross section of the repetitive unit cell (often called *non-self-intersecting condition*;
- some mechanical constraints on the effective material properties of the cellular core (to be used at the macro-scale);
- the geometric and feasibility constraints on the polar parameters of the laminated skins.

These aspects are detailed in the following subsections.

3.1 Geometrical design variables

Before introducing the geometric design variables characterising the sandwich panel at each scale, let us describe the Representative Volume Element (RVE) of the periodic cellular core. The RVE can be deduced from the geometry of the repetitive unit cell of the core which is characterised by three planes of orthogonal symmetry, as shown in Fig. 2. As illustrated in Fig. 3 the geometry of the RVE can be described in terms of both *global* and *local* geometric design variables. The global ones essentially represent the overall size of the RVE itself: h_c is the core height, t_c is the wall thickness, v_1 is the length of the free-shape oblique wall of the RVE along the η axis, while h_1 and h_2 are the lengths of the flat walls and of the middle region of the RVE along the ξ axis, respectively. In particular, the RVE can be inscribed within a parallelepiped having the following sizes:

$$a_1 = 2h_1 + h_2 \ , \quad a_2 = v_1 + t_c \ , \quad a_3 = \frac{h_c}{2} \ , \tag{1}$$

where a_1, a_2 and a_3 are the lengths of the edges along ξ, η and ζ axes, respectively. On the other hand, the local geometric design variables are needed in order to describe the shape of the middle region of the RVE. To this purpose, in this work the shape of the oblique wall of the RVE is represented in terms of a Non-Uniform Rational B-Spline (NURBS) curve [12] as:

$$\begin{aligned} \xi(s) &= \sum_{i=0}^{n_p} R_{i,p}(s)\,\xi_i, \\ \eta(s) &= \sum_{i=0}^{n_p} R_{i,p}(s)\,\eta_i, \\ \text{with } R_{i,p}(s) &= \frac{N_{i,p}(s)\,\omega_i}{\sum_{j=0}^{n_p} N_{j,p}(s)\,\omega_j} \quad 0 \le s \le 1 \ . \end{aligned} \tag{2}$$

Eq. (2) fully describes a pth-degree plane NURBS curve, as depicted in Fig 3. In particular, $\{\xi_i, \eta_i\}$ $(i = 0, \cdots, n_p)$ are the Cartesian coordinates of the ith control point (the set of control points forms the so-called *control polygon*), ω_i is the weight related to the ith control point, while $N_{i,p}(s)$ are the pth-degree B-spline basis functions defined on the non-periodic, non-uniform knot vector:

$$\mathbf{S} = \left\{ \underbrace{0, \cdots, 0}_{p+1}, S_{p+1}, \cdots, S_{m-p-1}, \underbrace{1, \cdots, 1}_{p+1} \right\} . \tag{3}$$

It is noteworthy that the dimension of the knot-vector is $m+1$ with $m = n_p + p + 1$. For a deeper insight in the matter the reader is addressed to [12]. In the present work the degree of the NURBS curve is $p = 3$, the number of control points has been chosen equal to ten (thus $n_p = 9$) and the B-spline basis functions are defined on the following non-periodic but uniform knot vector:

$$\overline{\mathbf{S}} = \left\{ 0, 0, 0, 0, \frac{1}{7}, \frac{2}{7}, \frac{3}{7}, \frac{4}{7}, \frac{5}{7}, \frac{6}{7}, 1, 1, 1, 1 \right\} . \tag{4}$$

In this background the shape of the oblique wall of the RVE can be modified by changing the positions of the points of the control polygon $\{\xi_i, \eta_i\}$ as well as the related weights ω_i. Therefore the previous parameters represent the local geometric design variables of the RVE. Of course, both global and local geometric design variables of the RVE of the core intervene at the meso-scale level. Since both kinds of geometrical parameters define the shape of the RVE a particular care must be taken in defining the position of the points of the control polygon. The coordinates of each point are defined as follows:

$$\begin{aligned} &\xi_i = h_1 + r_{\xi_i} h_2, \quad (i = 0, \cdots, n_p), \\ &\eta_i = r_{\eta_i} v_1. \end{aligned} \tag{5}$$

Where r_{ξ_i} and r_{η_i} are dimensionless parameters varying between zero and one. Moreover, in order to ensure C_0 continuity between the horizontal walls and the oblique part of the RVE the value of r_{ξ_i} and r_{η_i} must be fixed for the first and last point of the control net as follows:

$$\begin{aligned} &r_{\xi_0} = r_{\eta_0} = 0, \\ &r_{\xi_9} = r_{\eta_9} = 1. \end{aligned} \tag{6}$$

On the other hand, concerning the (identical) skins the only geometric design variable is the overall thickness h of the laminate. The geometric and material design variables together with their nature and bounds for the first-level problem are listed in Table 5. At this level of the optimisation procedure, the thickness of the laminated skins is considered as a discrete optimisation variable, the discretisation step being equal to the thickness of the elementary layer, i.e. $\Delta h = h_{\text{ply}}$ (see Table 5). This assumption responds to a technological constraint, and, in addition, the optimum value of this parameter will determine also the optimal number of layers n to be used during the second-level design problem. The geometric design variables intervening at the different scales can be grouped into the vector of the geometrical parameters defined as:

$$\mathbf{x_g} = \left\{ h, h_1, h_2, v_1, t_c, h_c, r_{\xi_0}, \cdots, r_{\xi_{n_p}}, r_{\eta_0}, \cdots, r_{\eta_{n_p}}, \omega_0, \cdots, \omega_{n_p} \right\} . \tag{7}$$

The geometric design variables involved within the first-level problem are not only limited by the box-constraints defined in Table 5, rather they have to meet also a certain number of requirements imposed to the problem at hand. Firstly, the shape of the cell must satisfy the non-self-intersecting condition: this constraint equation cannot be written in a close analytical form and can only be checked numerically (this check is automatically performed by the finite element code used to build the meso-scale model of the RVE). Secondly, the manufacturability constraint linked to the 3D printer (used to fabricate the prototype of the cellular core) must be considered. Such a constraint can be easily translated into a geometric constraint on the admissible ratio between the minimum radius of curvature of the oblique wall and the thickness of the walls of the RVE as:

$$g_1(\mathbf{x_g}) = 2t_c - \min(r(s)) \leq 0 , \tag{8}$$

where $r(s)$ is the local radius of curvature of the RVE. Finally, some further constraints must be considered to ensure the positive definiteness of the stiffness matrix of the cellular core (at the macro-scale) whose effective elastic properties depend on the geometric parameters of the RVE at the meso-scale. These constraints can be written as follows (see [19] for more details):

$$
\begin{aligned}
g_2(\mathbf{x_g}) &= -E_1^c < 0 \ , \\
g_3(\mathbf{x_g}) &= -E_2^c < 0 \ , \\
g_4(\mathbf{x_g}) &= -E_3^c < 0 \ , \\
g_5(\mathbf{x_g}) &= -G_{12}^c < 0 \ , \\
g_6(\mathbf{x_g}) &= -G_{13}^c < 0 \ , \\
g_7(\mathbf{x_g}) &= -G_{23}^c < 0 \ , \\
g_8(\mathbf{x_g}) &= |\nu_{12}^c| - \sqrt{\frac{E_1^c}{E_2^c}} < 0 \ , \\
g_9(\mathbf{x_g}) &= |\nu_{13}^c| - \sqrt{\frac{E_1^c}{E_3^c}} < 0 \ , \\
g_{10}(\mathbf{x_g}) &= |\nu_{23}^c| - \sqrt{\frac{E_2^c}{E_3^c}} < 0 \ , \\
g_{11}(\mathbf{x_g}) &= 2\nu_{12}^c\nu_{13}^c\nu_{23}^c\frac{E_3^c}{E_1^c} + (\nu_{12}^c)^2\,\frac{E_2^c}{E_1^c} + (\nu_{23}^c)^2\,\frac{E_3^c}{E_2^c} + (\nu_{13}^c)^2\,\frac{E_3^c}{E_1^c} - 1 < 0 \ .
\end{aligned}
\tag{9}
$$

E_1^c, E_2^c, E_3^c, G_{12}^c, G_{13}^c, G_{23}^c, ν_{12}^c, ν_{13}^c and ν_{23}^c are the effective material properties (engineering moduli) of the homogeneous orthotropic cellular core which are determined via the numerical homogenisation phase discussed in Section 5.1. It is noteworthy that the set of constraints of Eq. (9) are implicitly imposed on the geometric design variables (global and local) of the RVE.

3.2 Mechanical design variables

Concerning the mechanical design variables governing the behaviour of the laminated skins (at the macro-scale) the polar formalism has been employed. This method gives a representation of any planar tensor by means of a complete set of independent invariants, i.e. the *polar parameters*. It can be proved that in the case of a *fully orthotropic*, *quasi-homogeneous* laminate the overall number of independent mechanical design variables describing the elastic response of each laminated skin reduces to only three [10]: the anisotropic polar parameters $R_{0K}^{A^*}$ and $R_1^{A^*}$ and the polar angle $\Phi_1^{A^*}$ (this last representing the orientation of the main orthotropy axis) of the homogenised membrane stiffness tensor $\mathbf{A}^*$. For more details on the mechanical design variables intervening within the first-level problem the reader is addressed to [10].

In addition, in the formulation of the optimisation problem for the first level of the strategy, the geometric and feasibility constraints on the polar parameters (which arise from the combination of the layer orientations and positions within the stack) must also be considered. These constraints ensure that the optimum values of the polar parameters resulting from the first step correspond to a feasible laminate that will be designed during the second step of the optimisation strategy, see [20]. Since the laminate is quasi-homogeneous, such constraints can be written only for tensor $\mathbf{A}^*$ as follows:

$$\begin{cases} -R_0 \leq R_{0K}^{A^*} \leq R_0 \ , \\ 0 \leq R_1^{A^*} \leq R_1 \ , \\ 2\left(\dfrac{R_1^{A^*}}{R_1}\right)^2 - 1 - \dfrac{R_{0K}^{A^*}}{R_0} \leq 0 \ . \end{cases} \tag{10}$$

The previous variables can be grouped into the vector of mechanical design variables as follows:

$$\mathbf{x_m} = \left\{\Phi_1^{A*},\ R_{0K}^{A*},\ R_1^{A*}\right\} \ . \tag{11}$$

First and second constraints of Eq. (10) can be taken into account as admissible intervals for the relevant optimisation variables, i.e. on $R_{0K}^{A^*}$ and $R_1^{A^*}$. Hence, the resulting feasibility constraint on the laminate polar parameters is:

$$g_{12}(\mathbf{x_m}) = 2\left(\frac{R_1^{A^*}}{R_1}\right)^2 - 1 - \frac{R_{0K}^{A^*}}{R_0} \leq 0 \ . \tag{12}$$

For a wide discussion upon the laminate feasibility and geometrical bounds as well as on the importance of the quasi-homogeneity assumption the reader is addressed to [20].

3.3 Mathematical statement of the problem

As previously said, the aim of the first level optimisation is the least-weight design of the sandwich panel satisfying, simultaneously, constraints of different nature. The design variables (both geometrical and mechanical) of the problem can be grouped into the following vector:

$$\mathbf{x} = \left\{\Phi_1^{A^*}, R_{0K}^{A^*}, R_1^{A^*}, h, h_1, h_2, v_1, t_c, h_c, r_{\xi_1}, \cdots, r_{\xi_{n_p}}, r_{\eta_1}, \cdots, r_{\eta_{n_p}}, \omega_1, \cdots, \omega_{n_p}\right\} \ . \tag{13}$$

Therefore the optimisation problem can be formulated as follows:

$$\min_{\mathbf{x}} \ W(\mathbf{x})$$

subject to:

$$\begin{cases} \lambda_{glob}^{ref} - \lambda_{glob}(\mathbf{x}) \leq 0 \ , \\ \lambda_{loc}^{ref} - \lambda_{loc}(\mathbf{x}) \leq 0 \ , \\ g_i(\mathbf{x}) \leq 0 \ , \text{ with } i = 1, \cdots, 12 \ , \\ + \text{ n.s. intersecting condition} \ . \end{cases} \tag{14}$$

where W is the weight of the sandwich plate, λ_{glob} is the first global buckling load of the sandwich structure while λ_{loc} is the first local buckling load of the core. λ_{glob}^{ref} and λ_{loc}^{ref} are, respectively, the global and local buckling loads determined on a reference structure having the same in-plane dimensions and boundary conditions than those of the sandwich plate that will be optimised, see Section 6.

3.4 Numerical strategy

Problem (14) is a non-linear, non-convex problem in terms of both geometrical and mechanical variables. Its non-linearity and non-convexity is due on one side on the nature of the objective function and on the other side on the optimisation constraints, especially the constraint on the global buckling load that is a high non-convex function in terms of both the orthotropy orientation (bottom and top laminates) and the shape of the unit cell of the core. In addition, the complexity of such a problem is also due to: a) the existence constraints imposed on the technical moduli of the cellular core, see. Eq. (9), b) the manufacturability constraint that can be translated into a geometrical constraint imposed on the ratio between the thickness and the minimum radius of curvature of the oblique wall of the RVE, see Eq. (8), c) the non-self-intersecting constraint on the midline of the oblique wall of the RVE. The previous constraints are highly non-convex functions of the geometrical parameters of the RVE. The total number of design variables is 39 while the total number of optimisation constraints is 15 (see Eq. (14)).

For the resolution of problem (14) the GA BIANCA [21, 14] coupled with both the meso-scale FE model of the RVE (used for numerical homogenisation of the cellular core as well as for the calculation of the local buckling load of the cell) and the macro-scale FE model of the sandwich panel for the buckling analysis of the structure has been employed, see Fig. 4. The GA BIANCA was already successfully applied to solve different kinds of real-world engineering problems, see for example [22, 23, 24, 25, 26, 27].

As shown in Fig. 4, for each individual at each generation, the numerical tool performs a FE-based homogenisation for the evaluation of the effective material properties of the core and a subsequent numerical evaluation of the first buckling load of the sandwich structure (at both meso-scale and macros-scale for determining the local and global buckling loads, respectively) along with its weight. The meso-scale FE model makes use of the geometrical parameters of the unit cell (given by BIANCA and elaborated by MATLAB® which generates the NURBS curve representing the midline of the oblique wall of the RVE of the core) in order to perform the numerical homogenisation of the core and also to calculate the local buckling load of its unit cell. Afterwards, the macro-scale FE model utilises the geometrical and mechanical design variables of the skins given by BIANCA together with the effective material properties of the core (resulting from the meso-scale FE model of the cell) to evaluate the global buckling load of the structure and its weight. Therefore, for

these purposes the GA BIANCA has been interfaced with both the commercial FE code ANSYS® and the code MATLAB®. The GA elaborates the results provided by the two FE models in order to execute the genetic operations. These operations are repeated until the GA BIANCA meets the user-defined convergence criterion.

The generic individual of the GA BIANCA represents a potential solution for the problem at hand. The genotype of the individual for problem (14) is characterised by only one chromosome composed of 39 genes, each one coding a component of the vector of the design variables, see Eq. (13).

4 Methematical formulation of the second-level problem

The second-level problem concerns the lay-up design of the laminated skins. Such a problem consists in determining at least one stacking sequence satisfying the optimum values of both geometric and polar parameters resulting from the first level of the strategy and having the elastic symmetries imposed on the laminate within the formulation of the first-level problem, i.e. quasi-homogeneity and orthotropy. In the framework of the polar formalism, this problem can be stated in the form of an unconstrained minimisation problem:

$$\min_{\boldsymbol{\delta}} \; I\left(f_i\left(\boldsymbol{\delta}\right)\right) \tag{15}$$

with

$$I\left(f_i\left(\boldsymbol{\delta}\right)\right) = \sum_{i=1}^{6} f_i\left(\boldsymbol{\delta}\right) \; . \tag{16}$$

where $\boldsymbol{\delta}$ is the vector of the layer orientations, i.e. the design variables of this phase, while $f_i\left(\boldsymbol{\delta}\right)$ are quadratic functions in the space of polar parameters, each one representing a requirement to be satisfied, such as orthotropy, uncoupling, etc. For the problem at hand the partial objective functions write:

$$f_1(\boldsymbol{\delta}) = \left(\frac{|\Phi_0^{A^*}(\boldsymbol{\delta}) - \Phi_1^{A^*}(\boldsymbol{\delta})|}{\pi/4} - K^{A^*(opt)} \right)^2 \; , \quad f_2(\boldsymbol{\delta}) = \left(\frac{R_0^{A^*}(\boldsymbol{\delta}) - R_0^{A^*(opt)}}{R_0} \right)^2 \; ,$$
$$f_3(\boldsymbol{\delta}) = \left(\frac{R_1^{A^*}(\boldsymbol{\delta}) - R_1^{A^*(opt)}}{R_1} \right)^2 \; , \quad f_4(\boldsymbol{\delta}) = \left(\frac{|\Phi_1^{A^*}(\boldsymbol{\delta}) - \Phi_1^{A^*(opt)}|}{\pi/4} \right)^2 \; , \quad f_5(\boldsymbol{\delta}) = \left(\frac{||\mathbf{C}(\boldsymbol{\delta})||}{||\mathbf{Q}||} \right)^2 \; ,$$
$$f_6(\boldsymbol{\delta}) = \left(\frac{||\mathbf{B}^*(\boldsymbol{\delta})||}{||\mathbf{Q}||} \right)^2 \; , \tag{17}$$

where $f_1\left(\boldsymbol{\delta}\right)$ represents the elastic requirement on the orthotropy of the laminate having the prescribed shape (imposed by the value of K^{A^*} provided by the first step of the procedure), $f_2\left(\boldsymbol{\delta}\right)$, $f_3\left(\boldsymbol{\delta}\right)$ and $f_4\left(\boldsymbol{\delta}\right)$ are the requirements related to the prescribed values of the optimal polar parameters resulting from the first-level problem, while $f_5\left(\boldsymbol{\delta}\right)$ and $f_6\left(\boldsymbol{\delta}\right)$ are linked to the quasi-homogeneity condition.

$I(f_i(\boldsymbol{\delta}))$ is a positive semi-definite convex function in the space of laminate polar parameters, since it is defined as a sum of convex functions, see Eqs. (16)-(17). Nevertheless, such a function is highly non-convex in the space of plies orientations because the laminate polar parameters depend upon circular functions of the layers orientation angles, see Eq. (**??**). Moreover, one of the advantages of such a formulation consists in the fact that the absolute minima of $I(f_i(\boldsymbol{\delta}))$ are known a priori since they are the zeroes of this function. For more details about the nature of the second-level problem see [23, 14, 28]. Concerning the numerical strategy for solving problem (15) the GA BIANCA has been employed to find a solution also for the second-level problem. In this case, each individual has a genotype composed of n chromosomes, one for each ply, characterised by a single gene coding the layer orientation. It must be pointed out that problem (15) must be solved only one time as the skins are identical.

As conclusive remark of this section, it must be highlighted the fact that each ply orientation can get all the values in the range [-89°, 90°] with a discretisation step of 1°. Such a step has been chosen in order to prove that laminates with given elastic properties (such as membrane/bending uncoupling, membrane orthotropy, etc.) can be obtained by abandoning the well-known conventional rules for tailoring the laminate stack (e.g. symmetric-balanced stacks) which extremely shrink the search space for problem (15). The true advantages in using "non-conventional" staking sequences consist in the fact that on one hand with a discretisation step of one degree for the plies orientations the GA can explore the overall design space of problem (15) and on the other hand it can find very general stacks (nor symmetric neither balanced) that fully meet the elastic properties resulting from the first step of the procedure with a fewer number of plies (hence lighter) than the standard stacks, see [23, 14].

5 Finite element models at different scales

The FE models used at the first-level of the strategy are built using the FE commercial code ANSYS®. The FE analyses are conducted to determine the value of the objective and constraint functions for each individual, i.e. for each point in the design space, at the current generation.

The need to analyse, within the same generation, different geometrical configurations (plates with different geometrical and material properties), each one corresponding to an individual, requires the creation of an *ad-hoc* input file for the FE code that has to be interfaced with BIANCA. The FE model must be conceived to take into account a variable geometry, material and mesh. Indeed, for each individual at the current generation the FE code has to be able to vary in the correct way the number of elements wherein the structure is discretised, thus a proper parametrisation of the model has to be achieved.

During the optimisation process of the first level of the strategy, for each individual, eight FE analyses must be performed (see Fig. 4): six static analyses and one linear buckling analysis on the FE model of the unit cell of the cellular core (in order to determine the effective material properties [9] and the first local buckling load) and a linear buckling analysis on the FE model of the whole sandwich panel.

5.1 Finite element model of the unit cell (meso-scale)

In order to accurately determine the first local buckling load of the cellular core and its effective elastic properties a linear buckling analysis and a numerical homogenisation phase have to be achieved, respectively. The FE model of the RVE is illustrated in Fig. 5. The model has been built by using the 20-node solid element SOLID186 with three Degrees Of Freedom (DOFs) per node.

Concerning the linear elastic buckling analysis on the RVE the displacement Boundary Conditions (BCs) listed in Table 2 have been considered, while a uniform distributed pressure has been applied on the face located at $\zeta = a_3$. On the other hand, the effective properties of the core are determined using the strain energy homogenisation technique of periodic media, see [29]. This technique makes use of the repetitive unit of the periodic structure to approximate its effective properties at the macro-scale level. As in [9] the nine independent components of the stiffness tensor $\mathbf{C}$ of the cellular core have been determined through six static analyses.

The corresponding BCs for each one of the six static analyses performed on the FE model of Fig. 5 are resumed in Tables 3 and 4. These BCs are imposed in order to satisfy the symmetries of the RVE and to generate a strain field in such a way that only one component of the strain tensor is different from zero for each static analysis. For a deeper insight in the matter the reader is addressed to [9, 30].

It is noteworthy that since a shape optimisation of the unit cell is achieved within the framework of the first-level problem, the meso-scale FE model of the RVE must be able to take into account for variable geometry and mesh. To this purpose the mesh tool of the ANSYS code has been modified in order to make it compatible with a NURBS-based representation of the geometry (all these operations have been implemented within the APDL language of the ANSYS code). Finally, it has been previously checked that a mesh having an average value of 52000 DOFs (four divisions through the cell thickness) is sufficient for estimating the effective elastic properties as well as the local buckling load of the RVE with a good accuracy.

5.2 Finite element model of the sandwich panel (macro-scale)

At the macro-scale the structure is modelled with a combination of shell and solid elements. In particular, the laminated skins are modelled using ANSYS SHELL281 elements with

8-nodes and six DOFs per node, and their mechanical behaviour is described by defining directly the homogenised stiffness tensors $\mathbf{A}^*$, $\mathbf{B}^*$ and $\mathbf{D}^*$. The equivalent solid representing the core is modelled using ANSYS SOLID186 elements having the material properties provided by the FE model of the RVE. Concerning the BCs of the macro-scale FE model, they are depicted in Fig. 6 and listed in Table 6. In particular, such BCs are applied on the edges of the skins and not on the core.

The compatibility of the displacement field between skins (modelled with shell elements) and core (modelled with solid elements) is achieved by using ANSYS CERIG rigid constraints (also called rigid beams) whose formulation is based upon a classical master-slave scheme, see [31] for more details. Rigid constraints are imposed on each node belonging to contiguous solid and shell elements as depicted in Fig. 6. In particular, rigid beams are defined between the nodes of the middle plane of the top (bottom) skin and the corresponding ones of the top (bottom) surface of the solid core. In this case the master nodes are those belonging to shell elements (the skins), while slave nodes are those belonging the top and bottom surfaces of the core.

Finally, before starting the optimisation process, a sensitivity study (not reported here for the sake of brevity) on the proposed FE model with respect to the mesh size has been conducted: it was observed that a mesh having 12088 DOFs, i.e. showing two divisions through the core thickness h_c, is sufficient to properly evaluate the first buckling load of the structure.

6 Studied cases and results

In order to show the effectiveness of the proposed approach two different cases have been studied. In both cases a bi-axial compressive load per unit length is applied on the skins edges (as shown in Fig. 6): in the first one the ratio between the compressive loads is $\frac{N_y}{N_x} = 0.5$ while in the second one is $\frac{N_y}{N_x} = 1$. Moreover, for each case two sub-cases have been considered: the first one wherein the shape of the unit cell of the core is designed using B-Spline curves and the second one, more general, where the optimal shape of the unit cell is obtained using NURBS curves. It should be pointed out that these sub-cases are considered in order to investigate which-one of the two mathematical representations employed to describe the shape of the oblique wall of the RVE leads the GA to find an optimal solution more efficient (in terms of weight and buckling loads) than the reference one.

Before starting the multi-scale optimisation process a reference structure must be defined in order to establish reference values for the weight and for both the local and global buckling loads of the panel: the material as well as the geometrical properties of the reference sandwich plate are listed in Table 7. One can notice that the reference structure

has identical skins composed of 32 plies with the stacking sequence listed in Table 7. The choice of the reference solution has been oriented towards a non-trivial configuration with a honeycomb core characterised by a unit cell having the typical dimensions of commercial honeycombs (a regular hexagonal cell whose sizes are taken from [32], see also [9] for the definition of the geometric parameters defining the RVE of the hexagonal cell)) and two very stiff skins. In fact, the weight and the stiffness properties (in terms of buckling load) of such a reference configuration are typical of real-world engineering applications (in other words the reference solution still represents a "good" compromise between weight and stiffness requirements).

Regarding the setting of the genetic parameters for the GA BIANCA used to solve both first and second-level problems they are listed in Table 8. Moreover, concerning the constraint-handling technique for the first-level problem the Automatic Dynamic Penalization (ADP) method has been employed, see [21]. For more details on the numerical techniques developed within the new version of BIANCA and the meaning of the values of the different parameters tuning the GA the reader is addressed to [14, 23].

6.1 Case 1.a: shape optimisation using B-spline curve, load case $N_y = 0.5N_x$

For this first example, since a B-spline curve is utilised to describe the shape of the oblique wall of the RVE cross-section, the number of design variables reduces from 39 to 29 (all of the weights ω_i are fixed and equal to one).

The optimal values of the geometric as well as mechanical design variables resulting from the first-level of the optimisation strategy are listed in Table 9. As it can be easily seen, the optimum configuration has a weight of 29.35 Kg (about 27% lower than that of the reference structure) with a first global buckling load of 1642.98 N/mm (about 5% higher than that of the reference one) and a first local buckling load of 684.88 MPa (about 37% higher than that of the reference one).

Let us consider now the second-level problem: the design of the laminate lay-up. Table 10 shows the best stacking sequences for all the studied cases. As in each numerical technique, the quality of solutions found by BIANCA can be estimated on the basis of a numerical tolerance, i.e. the residual. For a discussion on the importance of the numerical residual in problems of this type, the reader is addressed to [14, 28]. $I\left(f_i\left(\boldsymbol{\delta}\right)\right)$ is a non-dimensional function, thus the residual of the solution is a non-dimensional quantity too. The residual in the last column of Table 10 is the value of the global objective function $I\left(f_i\left(\boldsymbol{\delta}\right)\right)$ for the solution indicated aside (we remind that exact solutions correspond to the zeroes of the objective function, see [28]). From Table 10 one can see that the optimal stacks (for all cases) are very general stacks which completely satisfy the elastic requirements of the laminate expected by problem 15. In fact, for this first case Fig. 7 shows

the first component of the homogenised stiffness tensors of the laminate, i.e. $\mathbf{A}^*$, $\mathbf{B}^*$ and $\mathbf{D}^*$: the solid line refers to the membrane stiffness tensor, the dashed one to the bending stiffness tensor, while the dash-dotted one is linked to the membrane/bending coupling stiffness tensor. It can be noticed that the laminate is uncoupled as the dash-dotted curve is reduced to a point in the center of the plot (B_{11} is practically null), homogeneous as the solid and dashed curves are almost coincident and orthotropic because there are two orthogonal axes of symmetry in the plane. In addition, the main orthotropy axis for this case is oriented at $\Phi_1^{A^*} = 83°$ as indicated in Table 9.

6.2 Case 1.b: shape optimisation using NURBS curve, load case $N_y = 0.5N_x$

In this sub-case a NURBS curve is considered for describing the shape of the oblique wall of the RVE cross-section, hence, the number of design variables is equal to 39 (all of the weights ω_i are included within the vector of design variables).

The optimal values of geometric as well as mechanical design variables of the first level problem are listed in Table 9. The optimum configuration weighs 28.63 Kg (a reduction of 29% when compared to that of the reference structure) with a first global buckling load of 1574.91 N/mm (1.2% greater than the reference one) and a local bukling load of 585.57 MPa (17% greater than the reference one).

This solution, as expected, is lighter than that of the case 1.a with a difference of 0.72 Kg with a lower value of both global and local buckling loads. This difference is due exclusively to the weight contribution given by the core. In fact, the optimum configuration of the panel for this case is characterised by two laminated skins which are as thick as those of the panel solution of case 1.a (2.50 mm, i.e. 20 plies); on the other hand the core shape is different and it is lighter than that characterising solution 1.a.

In addition, the weight reduction of the core has led to a reduction of the buckling load of the panel (both global and local) and, therefore, to a more compliant structure when compared to the solution 1.a. Of course, the variation of the shape of the unit cell together with the variation of the polar parameters of the skins occur in order to meet the prescribed minimal stiffness of the whole structure (at each scale) through the constraint on the first buckling loads.

Concerning the second-level problem, Table 10 shows the best stacking sequences for both the skins for the present case, while Fig. 8 shows the polar diagram for the first component of the corresponding homogenised stiffness tensors. Regarding the nature of the optimal stacks, even for this case, the same considerations as those of case 1.a can be repeated here.

6.3 Case 2.a: shape optimisation using B-spline curve, load case $N_y = N_x$

In this first sub-case a B-spline curve is employed to describe the shape of the oblique wall of the RVE cross-section. As in the case 1.a, this implies a reduction of the number of design variables that passes from 39 to 29 when compared to the most general case.

The optimal values of geometric and mechanical design variables resulting from the first-level of the optimisation strategy are listed in Table 9. The optimum configuration has a weight of 29.98 Kg (about 25.5% lower than that of the reference structure) with a first global buckling load of 1297.73 N/mm (1.1% greater than the reference one) and a local buckling load of 664.59 MPa (32.7% greater than the reference one).

In this case, the skins have the same weight of those of solutions of cases 1.a and 1.b , while the core is heavier than those of solutions 1.a and 1.b. Moreover, the core is heavier than its reference counterpart of about 0.38 Kg, see Table 9. Thus, the weight reduction is exclusively due to the skins that in terms of geometrical characteristics of the structure is translated in a laminate thickness reduction (that passes from 4.00 mm for the reference solution to 2.50 mm for the present case). Finally it can be stated that the constraints on the first global and local buckling loads are satisfied thanks to the combination of the optimal material parameters of the skins and the shape of the core that has improved the stiffness of the panel.

Concerning the results of the second-level problem the optimal stack is listed in Table 10 while the related polar diagrams are depicted in Fig. 9. The considerations already done for the previous cases can be repeated *verbatim* for the present one.

6.4 Case 2.b: shape optimisation using NURBS curve, load case $N_y = N_x$

In this last example the shape of the oblique wall of the RVE is mathematically represented through a NURBS curve, thus the vector of design variables corresponds to that of Eq. (13).

The optimal values of geometric as well as mechanical design variables provided by the first level of the optimisation strategy are listed in the last column of Table 9. The optimum configuration has a weight of 28.94 Kg (about 28.1% lower than that of the reference structure) with a first global buckling load of 1284.69 N/mm (almost equal than the reference one) and a local buckling load of 534.68 MPa (6.7% greater than the reference one).

Concerning the results of the second-level problem the optimum stack for both skins is listed in Table 10, while the related polar diagram is depicted in Fig. 10.

For the rest, the considerations already done for all of the other cases can be repeated here.

6.5 General discussion of results

The following aspects, arising from the analysis of the optimal configurations of the sandwich panel provided by the first level of the procedure (see Table 9), deserve a particular attention:

1. for each loading case, the solution wherein the oblique wall of the RVE is represented by means of a NURBS curve is lighter than that obtained through a B-spline representation (this fact proves the true advantages in using a richer and more general mathematical representation of parametric curves like the NURBS one);

2. for all the optimal solutions the thickness of the skins is the same (i.e. the optimum number of plies is the same for each case), the difference in terms of the laminate stiffness among the configurations concerns only the values of the laminate polar parameters resulting at the end of the first step. Accordingly, the optimal stacking sequences at the end of the second step are considerably different (see Table 10);

3. the reference solution of Table 7 is characterised by a shape of orthotropy with $K^{A^*} = 1$ (the value of $R_{0K}^{A^*}$ is negative), whilst the optimal configurations show different kinds of orthotropy (see Table 9 and Figs. 7 to 10): the solution of case 1.a is characterised by the same shape of orthotropy as the reference one, the laminate stiffness tensors of solutions 1.b and 2.a show an ordinary orthotropy with $K^{A^*} = 0$ (the corresponding value of $R_{0K}^{A^*}$ is positive) while solution 2.b is characterised by a square symmetric membrane stiffness tensor (the value of $R_1^{A^*}$ is negligible when compared to its lamina counterpart, i.e. R_1). Indeed, this means that, for the same loading conditions, laminates with different shapes of orthotropy are equivalent "potential" solutions for the problem at hand (this results represents also an evidence of the non-convexity of the optimisation problem);

4. for each solution the global design variables "tuning" the shape of the oblique wall of the RVE, i.e. h_2 and v_1, reach the upper bound, while the wall thickness t_c gets the lower bound: this means that the RVE shows a tendency of filling the available space by maximising the air volume restrained within the unit cell (and by minimising, simultaneously, the overall mass of the core itself);

5. the height of the core h_c gets the value of 38 mm for the solution of cases 1.a, 2.a and 2.b while its value decrease to 36 mm for the solution of case 1.b, i.e. for each configuration the optimum value of h_c lies almost in the middle of the definition interval. Indeed, this result is consistent: a high value of h_c would imply a decrease in the local buckling load and an increase in the global one, whereas a low value of h_c would cause the converse phenomenon. The optimum value of h_c represents a compromise between these two opposite responses;

6. for each solution the height of the core h_c is higher than that of the reference one, however the resulting local buckling load is always considerably higher than the reference value (37%, 17%, 32.7% and 6.7% for cases 1.a, 1.b, 2.a and 2.b, respectively). This result is due to the effect of the local geometric design variables (i.e. position of the control points and weights of the NURBS curve) tuning the shape of the oblique wall of the RVE: for each optimal configuration the shape of the wall show one or more "nodal" lines which increase the local buckling load of the unit cell, as depicted in Fig. 11;

7. the optimal configurations of the sandwich panel (for each considered case) show a slight increase in the global buckling load when compared to the reference solution although the overall thickness of the laminated skins strongly decreases. This fact is due, on one hand, to the higher value of h_c which increases the distance between the skins (thus the flexural stiffness of the panel), while, on the other hand, the skins get a more efficient combination of the laminate polar parameters (when compared to the reference solution): the union of these facts engenders a slight increase in the global buckling load of the sandwich panel.

In order to prove that the technological constraints (linked to the fabrication process) have been properly considered within the optimisation process and that the resulting complex (optimal) shapes can be really manufactured, two prototypes of the cellular core were fabricated. Such prototypes have been realised using the 3D printer described in Section 2.3. In particular, Fig. 11 presents both the Computer Aided Design (CAD) model and the related prototype of the cellular core for the optimal solutions of case 1.a and case 2.a. It is noteworthy that the prototype matches very well (i.e. within the technological tolerances) the CAD model of the core. Moreover, unlike the vast majority of shape and topology optimisation techniques employed for industrial purposes [33, 34] the proposed strategy does not need of a further step for the reconstruction of the CAD geometry, because the NURBS-based representation of the geometry of the cell is totally compatible with several standard file formats (IGES, STL and STEP) which easily allow the digital exchange of information among CAD systems.

7 Conclusions

The design strategy presented in this paper is a numerical optimisation procedure characterised by several features that make it an innovative, effective and general method for the multi-scale design of complex structures. In the present work this strategy has been employed to deal with the problem of the simultaneous shape and material optimisation of a sandwich panel composed of two laminated skins and a cellular core.

On one hand, the design process is not submitted to restrictions: any parameter characterising our structure is an optimisation variable. This allows the designer to look for a *true global minimum*, hard to be obtained otherwise. The formulation of the design problem of the sandwich panel is generalised and enriched by considering the shape optimisation of the unit cell of the core instead of the classical size optimisation of a prescribed geometry.

On the other hand, the multi-scale design problem has been split into two distinct but linked non-linear minimisation problems which are solved within the same procedure developed on two different levels. The first level of the procedure involves two different scales: the macro-scale of the sandwich panel composed of two homogeneous anisotropic plates (the skins) and of an homogeneous anisotropic core and the meso-scale of the cellular core modelled through its representative volume element. Many types of design variables are involved within this first level: the geometrical parameters (local and global) governing the shape of the unit cell (meso-scale) together with the geometric and material parameters of each skin (macro-scale). The second level of the procedure concerns the meso-scale of the laminated skins: in this phase, the goal consists in finding at least one optimal stack meeting on one hand the elastic requirements imposed to the laminate (quasi-homogeneity and orthotropy) and on the other hand the optimum value of the laminate polar parameters resulting from the first step.

Moreover, one of the main purposes of this work consists in proving that complex shapes of the cellular core can be really designed and manufactured (with the current technological capabilities): of course, this ambitious aim can be reached only by including, since the early stages of the design process, the manufacturability constraints linked to the considered fabrication process. To these purposes the two-level optimisation procedure has been enriched by considering the technological constraints linked to the 3D printer (chosen for fabricating the prototype of the unit cell) within the first level of the strategy. Concerning the topology of the cellular core, the shape of the unit cell is described by means of NURBS curves. The utilisation of NURBS blending functions allows for easily translating the manufacturability constraints into geometrical constraints to be imposed on the geometry of the representative unit cell. A further advantage linked to the utilisation of a NURBS-based representation of the geometry to be optimised is in the fact that NURBS curves and surfaces are totally compatible with the most used standard file formats (IGES, STL and STEP) in CAD systems. This aspect is of paramount importance because it allows to suppress from the design procedure further steps for the reconstruction of the CAD geometry that are often needed with usual shape and topology optimisation techniques.

Concerning the numerical computations, they are carried out by a genetic algorithm, BIANCA, able to handle both continuous and discrete-valued variables during the same calculation and to effectively handle the constraints of the problem. For the solution of the first-level problem, the code BIANCA is interfaced with the FE code ANSYS that invokes

eight FE analyses (at different scales) in order to compute the objective as well as the constraint functions of the problem.

On the other hand, the mechanical characteristics of the laminated plates are represented by the polar formalism, a mathematical representation characterised by several advantages, namely to explicit elastic symmetries, elastic and geometric bounds, and to eliminate from the procedure redundant mechanical properties. In addition, the utilisation of polar formalism leads the designer to easily formulate the second-level problem by taking into account in a correct and elegant way the requirements on the elastic symmetries of the structure.

To our best knowledge, this is the first time that the problem of the least-weight design of a sandwich panel with a cellular core is formulated in a very general way, i.e. by abandoning the usual simplifying hypotheses and the standard rules, taking into account all geometrical and material parameters characterising the structure as design variables and considering, within the same procedure, two different scales (meso and macro).

The utilisation of an evolutionary strategy, along with the fact that the problem is stated in the most general case, allows to find some non-conventional configurations more efficient than the standard ones. In fact, the considered numerical examples prove that when standard rules for tailoring the laminate stacks are abandoned and all the parameters characterising the structure, at each scale, are included among the design process a significant weight saving can be obtained: up to 29% compared to that of the reference structure with enhanced mechanical properties (in terms of both local and global buckling loads).

Finally, the proposed solutions can be yet employed for industrial purposes as they can be fabricated with the current technological capabilities. These considerations remain still valid if the designer wants to include within the process constraints of different nature, e.g. on strength, yielding, delamination, etc. or if he wants to improve the mathematical model to be optimised (i.e. the numerical model simulating the mechanical response of the structure) by introducing the influence of geometrical imperfections, material as well as geometrical non-linearity, etc. All of these aspects can be easily integrated within the optimisation process without altering its overall architecture and they do not represent a limitation to the proposed strategy, on the contrary they could be an interesting challenge for future researches on real-life applications.

References

[1] H. G. Allen, Analysis and design of structural sandwich panels, Pergamon Press, 1969.

[2] S. N. Huang, D. W. Alspaught, Minimum weight sandwich beam design, AIAA Journal 12 (1974) 1617–1618.

[3] M. N. Velea, P. Wennhage, D. Zenkert, Multi-objective optimisation of vehicle bodies made of frp sandwich structures, Composite Structures 111 (2014) 75–84.

[4] H. Asadi, M. Gorji, D. Ashouri, A. Khalkhali, Post buckling modelling and optimization of sandwich panels with corrugated cores, in: 5th WSEAS / IASME International Conference on ENGINEERING EDUCATION, Heraklion, Greece, 2008.

[5] M. M. Neves, H. Rodrigues, J. M. Guedes, Optimal design of periodic linear elastic microstructures, Computers and Structures 76 (2000) 421–429.

[6] C. Barbarosie, A. Toader, Shape and topology optimization for periodic problems, Structural and Multidisciplinary Optimization 40 (2010) 381–391.

[7] H. N. G. Wadley, N. A. Fleck, A. G. Evans, Fabrication and structural performance of periodic cellular metal sandwich structures, Composites Science and Technology 63 (2003) 2331–2343.

[8] X. Huang, Y. M. Xie, Optimal design of periodic structures using evolutionary topology optimization, Structural and Multidisciplinary Optimization 36 (2008) 597–606.

[9] A. Catapano, M. Montemurro, A multi-scale approach for the optimum design of sandwich plates with honeycomb core. Part I: homogenisation of core properties, Composite Structures 118 (2014) 664–676.

[10] A. Catapano, M. Montemurro, A multi-scale approach for the optimum design of sandwich plates with honeycomb core. Part II: the optimisation strategy, Composite Structures 118 (2014) 677–690.

[11] P. Vannucci, Plane anisotropy by the polar method, Meccanica 40 (2005) 437–454.

[12] L. Piegl, W. Tiller, The NURBS Book, Springer-Verlag, 1997.

[13] G. Verchery, Les invariants des tenseurs d'ordre 4 du type de l'élasticité, Proc. of colloque Euromech 115, VIllard-de-Lans, (France), 1979.

[14] M. Montemurro, Optimal design of advanced engineering modular systems through a new genetic approach, Ph.D. thesis, UPMC, Paris VI, France, http://tel.archives-ouvertes.fr/tel-00955533 (2012).

[15] S. W. Tsai, T. Hahn, Introduction to composite materials, Technomic, 1980.

[16] L. J. Gibson, M. F. Ashby, Cellular solids - Structure and properties, Cambridge University Press, 1997.

[17] Stratasys, Objet 30Pro, 7665 Commerce Way, Eden Prairie, MN 55344, http://www.stratasys.com/3d-printers/design-series/objet30-pro.

[18] Stratasys, PolyJet Materials, 7665 Commerce Way, Eden Prairie, MN 55344, http://www.stratasys.com/materials/polyjet.

[19] R. M. Jones, Mechanics of composite materials, McGraw-Hill, 1975.

[20] P. Vannucci, A note on the elastic and geometric bounds for composite laminates, Journal of Elasticity 112 (2013) 199–215.

[21] M. Montemurro, A. Vincenti, P. Vannucci, The automatic dynamic penalisation method (ADP) for handling constraints with genetic algorithms, Computer Methods in Applied Mechanics and Engineering 256 (2013) 70–87.

[22] M. Montemurro, A. Vincenti, P. Vannucci, A two-level procedure for the global optimum design of composite modular structures - application to the design of an aircraft wing. Part 1: theoretical formulation, Journal of Optimization Theory and Applications 155 (1) (2012) 1–23.

[23] M. Montemurro, A. Vincenti, P. Vannucci, A two-level procedure for the global optimum design of composite modular structures - application to the design of an aircraft wing. Part 2: numerical aspects and examples, Journal of Optimization Theory and Applications 155 (1) (2012) 24–53.

[24] M. Montemurro, A. Vincenti, Y. Koutsawa, P. Vannucci, A two-level procedure for the global optimization of the damping behavior of composite laminated plates with elastomer patches, Journal of Vibration and Control 21 (9) (2013) 1778–1800.

[25] M. Montemurro, Y. Koutsawa, S. Belouettar, A. Vincenti, P. Vannucci, Design of damping properties of hybrid laminates through a global optimisation strategy, Composite Structures 94 (2012) 3309–3320.

[26] M. Montemurro, H. Nasser, Y. Koutsawa, S. Belouettar, A. Vincenti, P. Vannucci, Identification of electromechanical properties of piezoelectric structures through evolutionary optimisation techniques, International Journal of Solids and Structures 49 (13) (2012) 1884–1892.

[27] A. Catapano, Stiffness and strength optimisation of the anisotropy distribution for laminated structures, Ph.D. thesis, UPMC, Paris VI, France, http://tel.archives-ouvertes.fr/tel-00952372 (2013).

[28] M. Montemurro, A. Vincenti, P. Vannucci, Design of elastic properties of laminates with minimum number of plies, Mechanics of Composite Materials 48 (2012) 369–390.

[29] E. J. Barbero, Finite element analysis of composite materials, Taylor and Francis Group, 2008.

[30] A. Catapano, J. Jumel, A numerical approach for determining the effective elastic symmetries of particulate-polymer composites, Composites Part B: Engineering 78 (2015) 227–243.

[31] ANSYS, Inc., 275 Technology Drive, Canonsburg, PA 15317, ANSYS Mechanical APDL Modeling and Meshing Guide (2012).

[32] HexWeb honeycomb attributes and properties, Duxford, Cambridge, UK (1999).

[33] Altair Engineering, Inc., 1820 E. Big Beaver, Troy, Michigan, USA, OptiStruct 11.0 User Guide (2011).

[34] G. Allaire, F. Jouve, Minimum stress optimal design with the level set method, Engineering Analysis with Boundary Elements 32 (2008) 909–918.

Tables

Alluminium		Carbon-Epoxy	
Material properties			
E	70000 MPa	E_1	181000 MPa
ν	0.33	E_2	10300 MPa
ρ	2.7×10^{-6} Kg/mm^3	G_{12}	7170 MPa
		ν_{12}	0.28
		ρ_s	1.58×10^{-6} Kg/mm^3
		h_{ply}	0.125 mm
Polar parameters			
		T_0	26880 MPa
		T_1	24744 MPa
		R_0	19710 MPa
		R_1	21433 MPa
		Φ_0, Φ_1	0 deg

Table 1: Material properties of the aluminium foil of the core and of the carbon-epoxy laminae of the skins.

Nodes	U_ξ	U_η	U_ζ
$\xi = 0$	0	free	free
$\xi = a_1$	0	free	free
$\eta = 0$	free	free	free
$\eta = a_2$	free	free	free
$\zeta = 0$	free	free	0
$\zeta = a_3$	0	0	free

Table 2: Boundary conditions for the FE model of the RVE, linear elastic buckling analysis.

1^{st} load case				2^{nd} load case				3^{rd} load case			
Nodes	U_ξ	U_η	U_ζ	Nodes	U_ξ	U_η	U_ζ	Nodes	U_ξ	U_η	U_ζ
$\xi = 0$	0	free	free	$\xi = 0$	0	free	free	$\xi = 0$	0	free	free
$\xi = a_1$	u_1	free	free	$\xi = a_1$	0	free	free	$\xi = a_1$	0	free	free
$\eta = 0$	free	0	free	$\eta = 0$	free	0	free	$\eta = 0$	free	0	free
$\eta = a_2$	free	0	free	$\eta = a_2$	free	u_2	free	$\eta = a_2$	free	0	free
$\zeta = 0$	free	free	0	$\zeta = 0$	free	free	0	$\zeta = 0$	free	free	0
$\zeta = a_3$	free	free	0	$\zeta = a_3$	free	free	0	$\zeta = a_3$	free	free	u_3

Table 3: Boundary conditions for the FE model of the RVE: 1^{st}, 2^{nd} and 3^{rd} static analyses.

4^{th} load case				5^{th} load case				6^{th} load case			
Nodes	U_ξ	U_η	U_ζ	Nodes	U_ξ	U_η	U_ζ	Nodes	U_ξ	U_η	U_ζ
$\xi = 0$	0	free	free	$\xi = 0$	free	0	0	$\xi = 0$	free	0	0
$\xi = a_1$	0	free	free	$\xi = a_1$	free	0	u_3	$\xi = a_1$	free	u_2	0
$\eta = 0$	0	free	0	$\eta = 0$	free	0	free	$\eta = 0$	0	free	0
$\eta = a_2$	0	free	u_3	$\eta = a_2$	free	0	free	$\eta = a_2$	u_1	free	0
$\zeta = 0$	0	0	free	$\zeta = 0$	0	0	free	$\zeta = 0$	free	free	0
$\zeta = a_3$	0	u_2	free	$\zeta = a_3$	u_1	0	free	$\zeta = a_3$	free	free	0

Table 4: Boundary conditions for the FE model of the RVE: 4^{th}, 5^{th} and 6^{th} static analyses.

Design variable	Type	Lower bound	Upper bound	Discretisation step
R_{0K}^{A*} [MPa]	continuous	-19710.0	19710.0	-
R_1^{A*} [MPa]	continuous	0	21433.0	-
Φ_1^{A*} [deg]	discrete	-90	90	1
h [mm]	discrete	2.50	4.00	0.125
h_1 [mm]	discrete	1.00	4.00	0.1
h_2 [mm]	discrete	2.00	5.00	0.1
v_1 [mm]	discrete	2.00	5.00	0.1
t_c [mm]	discrete	0.20	0.40	0.01
h_c [mm]	discrete	20.00	60.00	1.00
r_{ξ_i}	discrete	0.00	1.00	0.01
r_{η_i}	discrete	0.00	1.00	0.01
ω_i	discrete	0.01	1.00	0.01

Table 5: Design space of the first-level problem.

Sides	BCs
AB, A′B′, CD, C′D′	$U_x = 0$
	$U_z = 0$
BC, B′C′, DA, D′A′	$U_y = 0$
	$U_z = 0$

Table 6: BCs of the FE model of the sandwich panel.

a, b [mm]	1500.00
Φ_1^{A*} [deg]	0.0
R_{0K}^{A*} [MPa]	-9855.21
R_1^{A*} [MPa]	5358.28
h [mm]	4.00
ϑ [deg]	60.00
l_2 [mm]	2.75
l_1 [mm]	5.50
t_c [mm]	0.25
h_c [mm]	30
Skins Weight [Kg]	28.44
Core weight [Kg]	11.82
Panel weight [Kg]	40.26
Buckling load (Case 1) [N/mm]	1556.43
Buckling load (Case 2) [N/mm]	1283.50
Local buckling load [MPa]	500.66
Stacking sequence	N. of plies
$[45/0/45/45/-45/45/-45/0/0/45/-45/45/-45/-45/0/45]_s$	32

Table 7: Reference solution for the sandwich panel design problem,(for the definition of the geometric parameters of the RVE of the hexagonal unit cell of the honeycomb core see [9, 10]).

Genetic parameters		
	1^{st} level problem	2^{nd} level problem
N. of populations	1	1
N. of individuals	160	500
N. of generations	200	500
Crossover probability	0.85	0.85
Mutation probability	0.00625	0.002
Selection operator	roulette-wheel	roulette-wheel
Elitism operator	active	active

Table 8: Genetic parameters of the GA BIANCA for both first and second-level problems.

	Solution case 1.a	Solution case 1.b	Solution case 2.a	Solution case 2.b
Φ_1^{A*} [deg]	83.00	47.00	44.00	49.00
R_{0K}^{A*} [MPa]	-6608.53	19555.90	19517.30	19517.30
R_1^{A*} [MPa]	9281.35	2891.26	4714.00	1613.24
h [mm]	2.50	2.50	2.50	2.50
h_1 [mm]	1.50	1.50	1.60	2.10
h_2 [mm]	5.00	5.00	5.00	4.90
v_1 [mm]	5.00	5.00	4.55	5.00
t_c [mm]	0.20	0.20	0.20	0.20
h_c [mm]	38.00	36.00	38.00	38.00
(ξ_0, η_0) [mm]	(1.50, 0.00)	(1.50, 0.00)	(1.60, 0.00)	(2.10, 0.00)
(ξ_1, η_1) [mm]	(2.05, 0.00)	(2.05, 0.00)	(2.15, 0.00)	(2.64, 0.00)
(ξ_2, η_2) [mm]	(2.61, 0.50)	(2.61, 0.50)	(2.71, 1.46)	(3.19, 1.55)
(ξ_3, η_3) [mm]	(3.17, 0.70)	(3.17, 0.70)	(3.27, 2.23)	(3.73, 2.20)
(ξ_4, η_4) [mm]	(3.72, 2.25)	(3.72, 2.25)	(3.82, 2.27)	(4.28, 3.40)
(ξ_5, η_5) [mm]	(4.28, 3.25)	(4.28, 3.25)	(4.38, 2.91)	(4.82, 3.45)
(ξ_6, η_6) [mm]	(4.83, 3.75)	(4.83, 3.75)	(4.93, 3.59)	(5.37, 3.60)
(ξ_7, η_7) [mm]	(5.39, 3.95)	(5.39, 3.95)	(5.49, 3.18)	(5.91, 4.30)
(ξ_8, η_8) [mm]	(5.94, 5.00)	(5.94, 5.00)	(6.04, 4.55)	(6.45, 5.00)
(ξ_9, η_9) [mm]	(6.50, 5.00)	(6.50, 5.00)	(6.60, 4.55)	(7.00, 5.00)
ω_0	1.00	0.63	1.00	0.40
ω_1	1.00	0.27	1.00	0.44
ω_2	1.00	0.72	1.00	0.72
ω_3	1.00	0.11	1.00	0.63
ω_4	1.00	0.70	1.00	0.10
ω_5	1.00	0.11	1.00	0.44
ω_6	1.00	0.70	1.00	0.26
ω_7	1.00	0.67	1.00	0.89
ω_8	1.00	0.42	1.00	0.51
ω_9	1.00	0.59	1.00	0.98
Skins Weight [Kg]	17.78	17.78	17.78	17.78
Core weight [Kg]	11.57	10.85	12.20	11.16
Panel weight [Kg]	29.35	28.63	29.98	28.94
Buckling load [N/mm]	1642.98	1574.91	1297.73	1284.69
Local buck. load [MPa]	684.88	585.57	664.59	534.68

Table 9: Numerical results of the fist-level optimisation problem for both 1^{st} and 2^{nd} cases.

	Best stacking sequence	N. of plies	Residual
Reference Solution	$[45/0/45/45/-45/45/-45/0/0/45/-45/45/-45/-45/0/45]_s$	32	
Case 1.a	$[36/-55/68/-74/79/-71/48/57/-55/-87/44/50/-57/-49/26/-74/90/54/60/-60]$	20	2.20×10^{-4}
Case 1.b	$[47/47/-43/-43/47/-43/47/-43/47/-43/-43/47/47/47/47/-43/-43/47/47/-43]$	20	3.96×10^{-4}
Case 2.a	$[-45/44/43/-48/-44/44/-45/60/35/44/-45/43/-47/-48/45/-41/-43/43/-48/46]$	20	3.18×10^{-4}
Case 2.b	$[-40/50/49/-44/48/48/-40/-41/-38/55/-40/-43/46/48/-44/48/49/50/-36/-44]$	20	3.94×10^{-4}

Table 10: Numerical results of the second-level optimisation problem for both 1^{st} and 2^{nd} cases.

Figures

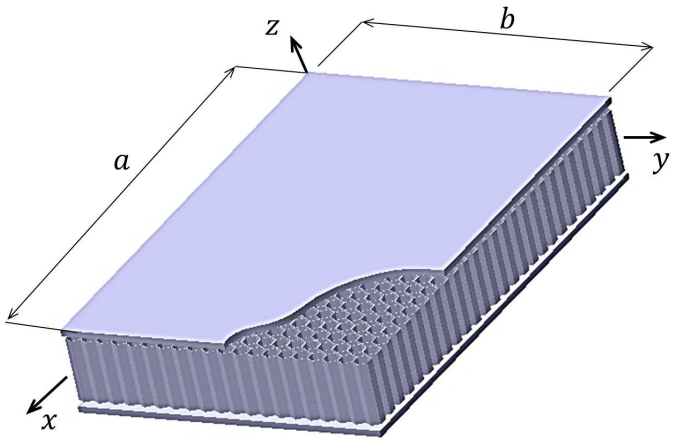

Figure 1: Geometry of the sandwich panel.

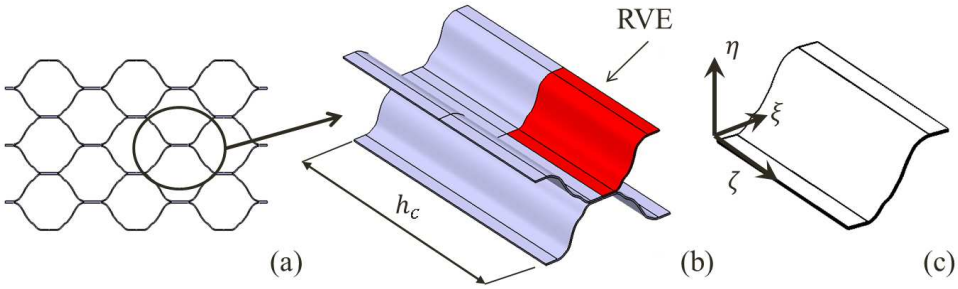

Figure 2: Honeycomb core structure (a), the repetitive unit cell (b) and the related RVE (c).

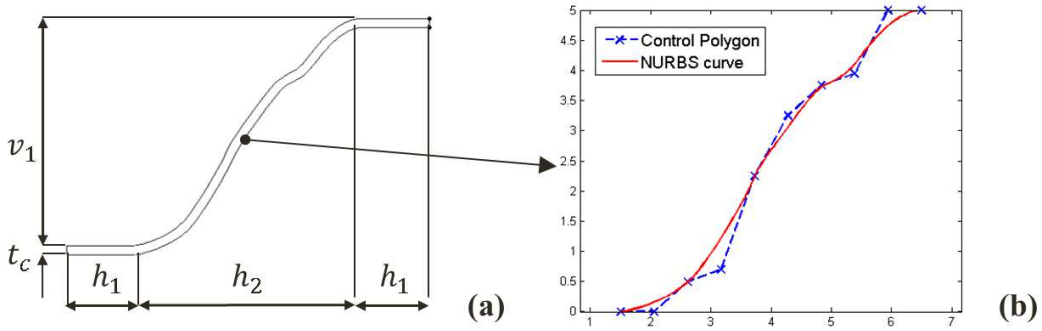

Figure 3: Global geometric design variables of the RVE (a) and the NURBS representation of the oblique wall of the RVE (b).

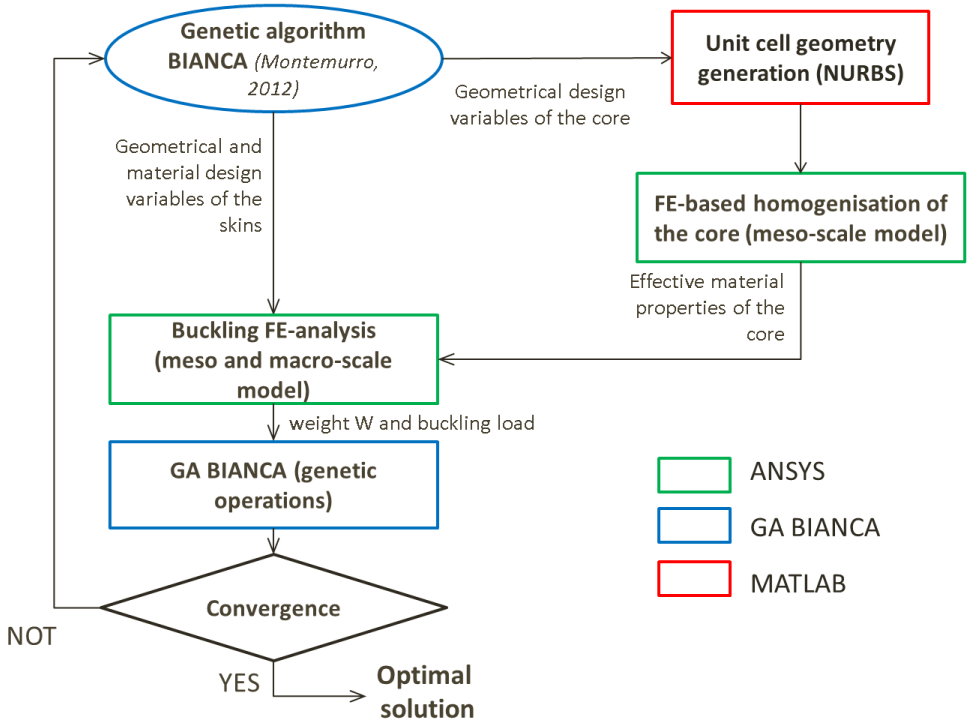

Figure 4: Logical flow of the numerical procedure for the solution search of the fist-level problem.

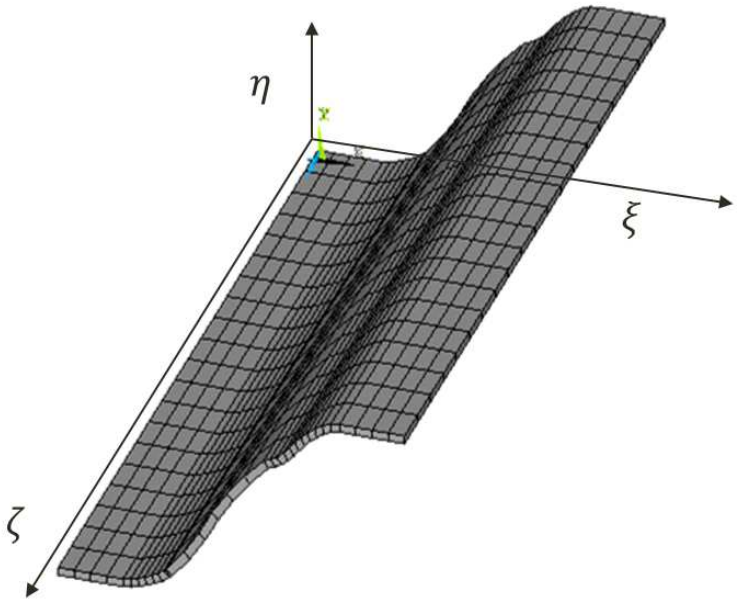

Figure 5: FE model of the RVE.

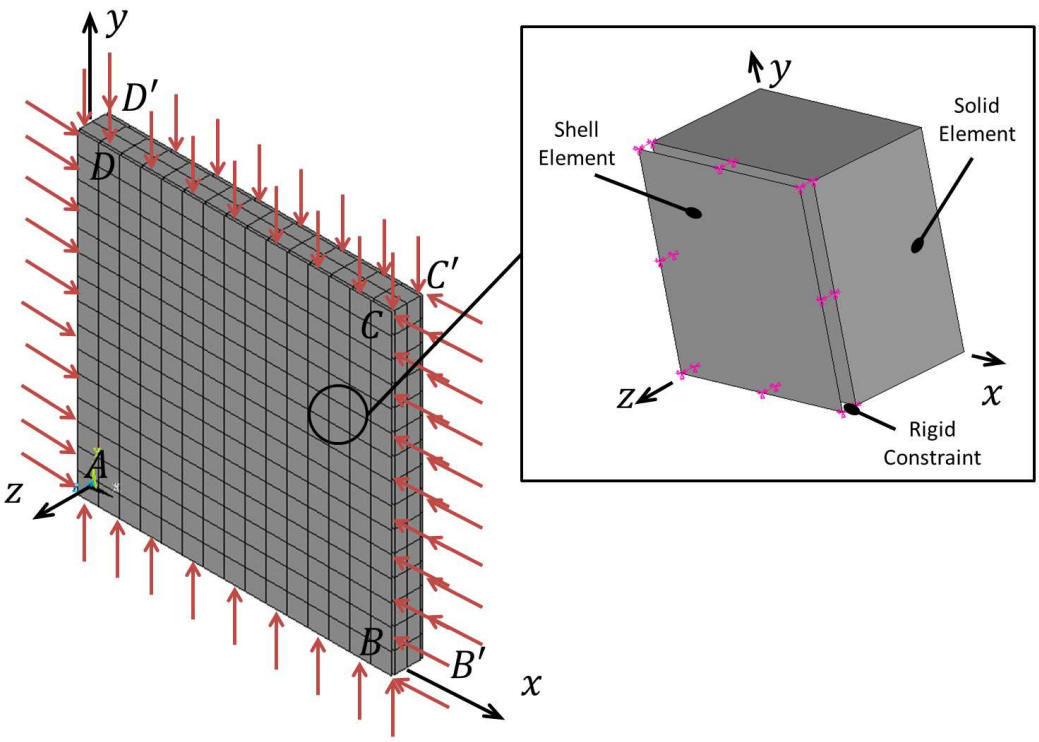

Figure 6: Mesh and rigid constraint equations for the FE model of the sandwich panel.

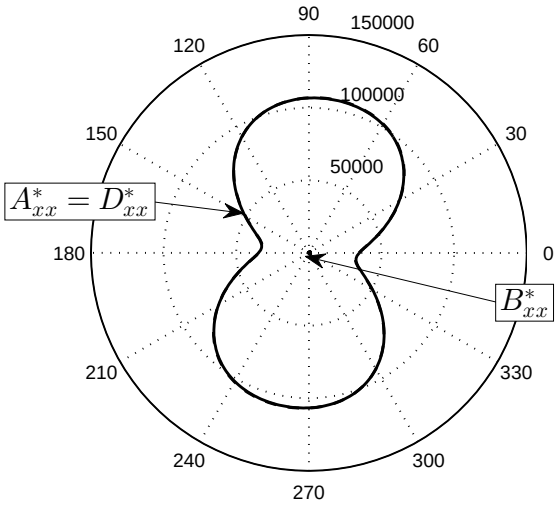

Figure 7: First component of the homogenised stiffness tensors of the laminate [MPa], case 1.a.

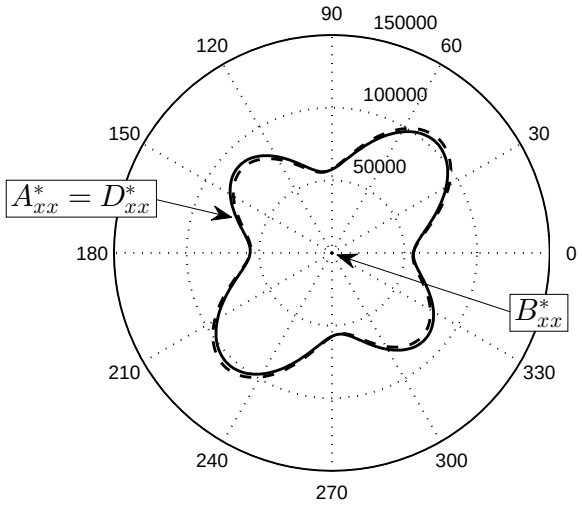

Figure 8: First component of the homogenised stiffness tensors of the laminate [MPa], case 1.b.

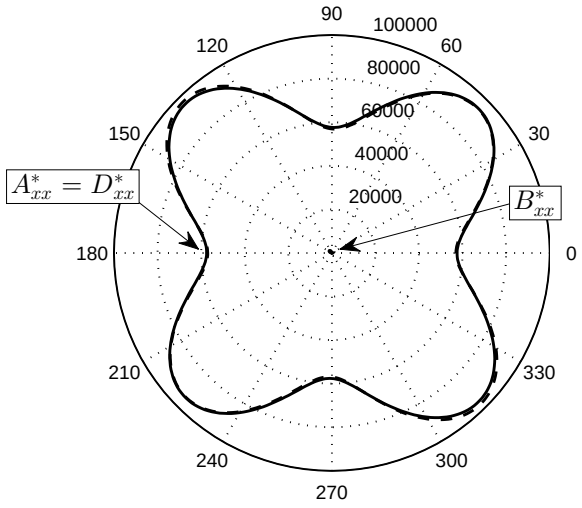

Figure 9: First component of the homogenised stiffness tensors of the laminate [MPa], case 2.a.

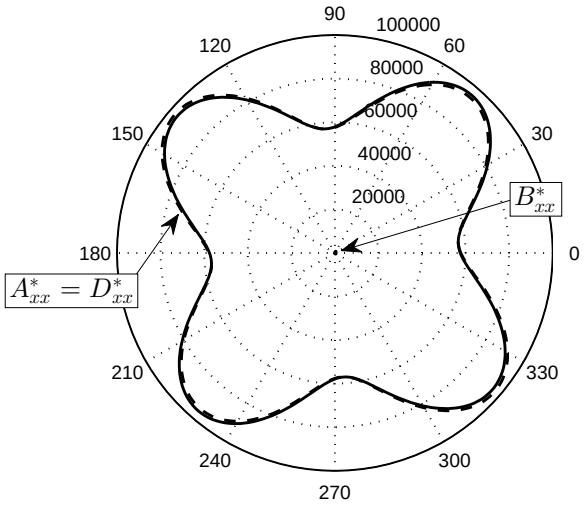

Figure 10: First component of the homogenised stiffness tensors of the laminate [MPa], case 2.b.

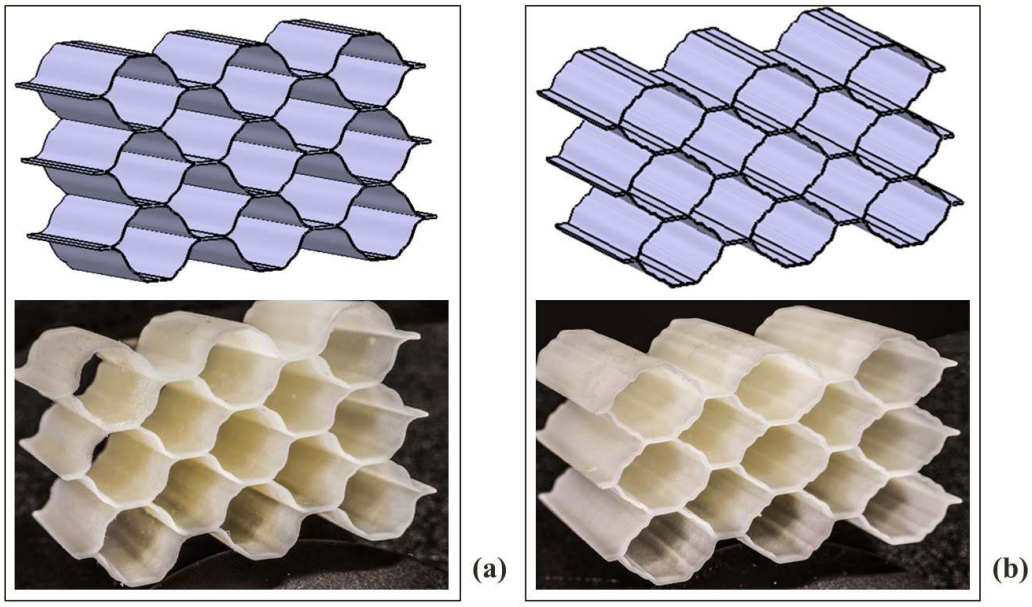

Figure 11: CAD and 3D printed prototypes of the cellular core for the optimal solution of case 1.a (a) and case 2.a (b).